EBioMedicine 70 (2021) 103537

Contents lists available at ScienceDirect

EBioMedicine

journal homepage: www.elsevier.com/locate/ebiom

The role of voltage-gated chloride channels in the epileptogenesis of temporal lobe epilepsy

Kai-Feng Shen[a], Xiao-Lin Yang[a], Guo-Long Liu[a], Gang Zhu[a], Zhong-Ke Wang[a], Xian-Jun Shi[a], Ting-Ting Wang[a], Zhi-Feng Wu[b], Sheng-Qing Lv[a], Shi-Yong Liu[a], Hui Yang[a], Chun-Qing Zhang[a,*]

[a] Department of Neurosurgery, Xinqiao Hospital, Army Medical University, 2-V Xinqiao Street, Chongqing 400037, China
[b] Department of Pediatrics, Xinqiao Hospital, Army Medical University, 2-V Xinqiao Street, Chongqing 400037, China

ARTICLE INFO

Article History:
Received 20 April 2021
Revised 18 July 2021
Accepted 29 July 2021
Available online xxx

Key words:
Temporal lobe epilepsy
Voltage-gated chloride channels
Chloride channel blockers
High-frequency oscillations

ABSTRACT

Background: Temporal lobe epilepsy (TLE) is the most common intractable epilepsy in adults, and elucidation of the underlying pathological mechanisms is needed. Voltage-gated chloride channels (ClC) play diverse physiological roles in neurons. However, less is known regarding their functions in the epilepogenesis of TLE.
Methods: ClC-mediated current and the spontaneous inhibitory synaptic currents (sIPSC) in hippocampal neurons of epileptic lesions were investigated by electrophysiological recording. The EEG data were analyzed by Z-scored wavelet and Fourier transformations. The expression of *ClC-3*, a member of ClC gene family, was detected by immunostaining and western blot.
Findings: ClC-mediated current was increased in the hippocampal neurons of chronic TLE mice. Application of chloride channel blockers, NPPB (5-Nitro-2- [3-phenylpropylamino] benzoic acid) and DIDS (4,4'-Diisothiocyanato-2,2'-stilbenedisulfonic acid disodium salt) reduced ClC-mediated current and increased inhibitory synaptic transmission in TLE mice. NPPB and DIDS reduced the seizure frequency and the average absolute power of ictal high-frequency oscillations (HFOs, 80-500 Hz) in TLE mice. In addition, both drugs induced outwardly rectified currents, which might be tonic inhibitory currents in the hippocampal neurons of TLE patients. Furthermore, the expression of ClC-3 was increased in the hippocampus of TLE mice and patients and positively correlated with both the absolute power and number of ictal HFOs per seizure in the sclerotic hippocampus.
Interpretation: These data suggest that ClC participate in the epilepogenetic process of TLE and the inhibition of ClC may have anti-epileptic effect.
Funding: This work was supported by National Natural Science Foundation of China (No. 81601143, No. 81771217).

1. Introduction

Epilepsy is a common chronic neurological disease that affects approximately 1% of the population worldwide. Temporal lobe epilepsy (TLE) is the most common type of epilepsy in adults. To date, TLE is mostly refractory to anti-epileptic drugs (AEDs) and ultimately requests surgical resection of the epileptogenic foci. [1] Thus, further mechanistic understanding of TLE is needed to develop novel strategies for the prevention and treatment of epilepsy in TLE patients.

Chloride is the most abundant anion in neurons and also the primary anion transported by $GABA_A$ receptors to introduce inhibitory synaptic transmission in the neuronal system. Many AEDs, such as benzodiazepine and barbiturate drugs have been developed to potentiate the function of GABA and $GABA_A$ receptors. In comparison, other channels involved in transmembrane chloride transportation during the epileptogenesis of TLE are less characterized. Voltage-gated chloride channels (ClC) are a group of chloride channels that have diverse physiological functions, such as blood pressure regulation, cell proliferation and apoptosis, cell volume regulation and neuronal excitability. Abnormalities of these channels have been shown to cause tissue-specific pathologies. [2-5] Nine different genes (*ClC-1* to *ClC-7*, and *ClC-Ka* and *ClC-Kb*) encoding for ClC have been identified in mammalian tissues, among which ClC-3, ClC-4 and ClC-5 are constitutively active in mediating outwardly rectifying current. [3] ClC-3

* Correspondence: Chun-Qing Zhang, MD, PhD. Department of Neurosurgery, Xinqiao Hospital, Army Medical University, 2-V Xinqiao Street, Chongqing 400037, China. Phone: +86-23-68774010, Fax: +86-23-65218204.
E-mail address: cqzhang@tmmu.edu.cn (C.-Q. Zhang).

https://doi.org/10.1016/j.ebiom.2021.103537

Research in context

Evidence before this study

Temporal lobe epilepsy (TLE) is the most common intractable epilepsy in adults and approximately 30% of TLE patients do not respond adequately to exiting anti-epileptic drugs (AEDs). Voltage-gated chloride channels (ClC) have diverse physiological functions such as regulating neuronal excitability; however, their roles in the epileptogenesis of TLE remain obscure.

Added value of this study

In the present study, we presented evidence that ClC are significantly involved in the epileptogenesis of TLE. ClC-mediated outwardly rectified current was increased in the hippocampal neurons of chronic TLE mice and led to the elevation of intracellular chloride concentration in the neurons of epileptogenic lesions. Chloride channel blockers NPPB and DIDS efficiently reduced ClC-mediated current and increased the inhibitory transmission in hippocampal neurons of TLE mice. *In vivo* study found that NPPB and DIDS reduced the seizure frequency and the power of ictal HFOs in the hippocampus of chronic TLE mice. Additionally, NPPB and DIDS induced an outward current, which was likely a tonic inhibitory current in the hippocampal neurons of intractable TLE patients. Furthermore, we identified *ClC-3*, a ClC gene family member, had higher expression in the hippocampus of TLE mice and TLE patients, and its expression was positively correlated with both the power and number of ictal HFOs per seizure in the sclerotic hippocampus. These characterizations of the relations between ClC and TLE advance the understanding of the mechanism of epileptogenesis in TLE.

Implications of all the available evidence

This study reveals the potential role of ClC in the epileptogenesis of TLE with evidence from chronic TLE mice and TLE patients and suggests that ClC might be a potential anti-epileptic target.

and ClC-4 are the two major members expressed in the brain, and whereas ClC-4 is known to locate predominantly in intracellular membranes, the function of ClC-3 in the brain is much less known. [6,7] Previous studies found that *ClC-3* knockout mice displayed a selective hippocampus degeneration and spontaneous generalized tonic-clonic seizures, which are similar to the pathological process of sclerotic hippocampus in TLE. [8,9] Although these evidence suggest that ClC might be involved in the epileptogenesis of TLE, detailed mechanistic studies are further needed to understand how this chloride channel type governs electrophysiological events therein and what would be the possible targeting strategy.

Here, by using a chronic TLE animal model and TLE patient specimens, we investigated ClC-mediated outwardly rectified currents in the hippocampal neurons and the effects of chloride channel blockers including NPPB (5-Nitro-2- [3-phenylpropylamino] benzoic acid) and DIDS (Diisothiocyanato-2,2′-stilbenedisulfonic acid disodium salt) on the inhibitory synaptic transmission in hippocampal neurons. Additionally, we examined the effects of NPPB and DIDS on seizure activity by *in vivo* mouse experiments. Furthermore, we characterized the expression of *ClC-3* in the epileptogenic hippocampus of TLE animals and patients, and analyzed the correlation of ClC-3 protein abundances with clinical variables, including the frequency and power of ictal high-frequency oscillations (HFOs, 80-500 Hz) in hippocampal lesions, seizure duration before surgery, seizure frequency and types of AEDs taken in TLE patients.

2. Methods

2.1. Human specimens

The human brain tissues were obtained from the Department of Neurosurgery of Xinqiao Hospital (Army Medical University, Chongqing, China). Human samples were collected from fully informed individuals who provided written consent. Fifteen human sclerotic hippocampus specimens were collected from patients diagnosed with intractable TLE according to the criteria established by the International League Against Epilepsy (ILAE), [10] and the detailed information was illustrated in Table 1. Due to the sparsity of age-matched control hippocampal specimens, the control hippocampal specimens were collected from five autopsies of age-matched individuals without a known history of neurologic or psychiatric disease, ensuring a 3:1 disease-to-control match. All tissues were collected within six hours after death when most proteins were stable in this postmortem interval. [11] The average age of the intractable TLE patients was 26.20 ± 1.49 years (range: 18−37 years), with 8 males and 7 females. The control group consisted of 2 female and 3 male individuals with an age of 31.80 ± 4.60 years (range: 21-43 years), and the basic information was illustrated in Table 2. No significant difference in age or gender was found between TLE patients and the controls. The studies were performed in accordance with the guidelines of Army Medical University and with the ethical standards in Helsinki declaration. [12]

2.2. Animals

Adult male C57BL/6J mice aged 2-3 months were randomly assigned to different groups according to a computer-generated sequence in the study. Animals were housed under standard conditions (room temperature, 23 ± 1°C; illumination, 12-hour light/12-hour dark cycle; access to food and water, *ad libitum*). All the animal experimental procedures were reviewed and approved by the Internal Animal Care and Use Committee of the Army Medical University.

2.3. Electrophysiological recording

Slice preparation and electrophysiological recordings were performed in a similar way to our previous study. [13] Control or TLE mice were anesthetized with phenobarbital sodium (60 mg/kg, i.p.) and the brains were rapidly decapitated, removed and placed in an ice-cold sucrose-based dissecting solution (in mM): sucrose (300), KCl (2), NaH_2PO_4 (1.25), $CaCl_2$ (1), $MgCl_2$ (5), $NaHCO_3$ (26) and glucose (11). The tissue blocks with hippocampus were trimmed and cut into transverse slices (300 μm) with a vibrating microtome (Leika, VT1000 S, Germany) in a cold bubbled sucrose-based solution, and transferred to an oxygenated recovery chamber containing standard artificial cerebrospinal fluid (ACSF) (in mM): NaCl (140), KCl (2.5), NaH_2PO_4 (1.4), $CaCl_2$ (2), $MgCl_2$ (2), $NaHCO_3$ (25) and glucose (11) at 35°C for 30 min and then used for recording. The freshly dissected sclerotic hippocampus of TLE patients was cut into slices with the same procedure after transportation from operating room to laboratory in bubbling oxygenated ice-cold dissecting solution in 5-10 min after resection.

Voltage-gated chloride currents in the CA1 pyramidal neurons were evoked from a holding potential of -60 mV to the test pulses ranging from −100 to +100 mV by an increment of 20 mV at an interval of 5 s following a previous published procedure. [14] The external solution contained (in mM): NMDG-Cl (135), HEPES (20), Glucose (20), $MgSO_4$ (2) and $CdCl_2$ (200), tetrodotoxin (TTX, 500 nM) and 4-aminopyridine (4-AP, 1 mM) were included in the bath solution to block sodium and potassium currents, bicuculline (20 μM) was applied to block $GABA_A$ receptors, 300 mOsm, pH 7.3−7.4 adjusted by CsOH. The normal chloride pipette solution contained (in mM):

Table 1
Information about TLE patients.

Subjects	Gender	Age(year)	Course(year)	AEDs before surgery	Seizure type	Frequency per month	Resected tissue	Pathology	Application used
1	F	18	14	CBZ, VPA,TPM	FBTCS	35	RTN, RH	G	WB, IHC, IF
2	F	37	8	VPA, PHT	FAS	20	RTN, RH	G	WB, IHC, EP
3	M	32	12	OXC, VPA	FAS	104	RTN, RH	G	WB, IHC
4	F	25	8	TPM, CLB	FAS	64	LTN, LH	NL	WB, IHC, IF
5	M	21	11	OXC, VPA	FIAS	90	LTN, LH	G, NL	WB, IHC
6	M	23	11	VPA, PHT, PB, CBZ	FIAS	153	RTN, RH	G	WB, IHC, EP
7	M	24	18	PHT, VPA	FIAS	35	LTN, LH	G, NL	WB, IHC, EP
8	M	19	12	VPA, OXC, LEV	FIAS	30	LTN, LH	G	WB, IHC
9	F	31	15	VPA, OXC, TPM	FAS	92	RTN, RH	G	WB, IHC
10	F	25	22	LTG, VPA, LEV	FBTCS	31	LTN, LH	G, NL	WB, IHC
11	M	20	9	VPA, PHT, PB	FIAS	118	RTN, RH	G, NL	WB, IHC
12	M	28	14	VPA, PHT, PB	FAS	43	RTN, RH	G	WB, IHC, EP
13	M	25	12	VPA, TPM, PB	FAS	16	LTN, LH	NL	WB, IHC, IF
14	F	31	9	CBZ, CLB, PHT	FBTCS	39	RTN, RH	G	WB, IHC, EP
15	F	34	17	LTG, TPM, PB	FAS	42	RTN, RH	ND	WB, IHC, EP

M, male; F, female; AED, anti-epileptic drugs; CBZ, carbamazepine; VPA, valproic acid; CLB, clonazepam; LTG, lamotrigine; OXC, oxcarbazepine; PB, phenobarbital; PHT, phenytoin; TPM, topiramate. FIAS, focal impaired awareness seizure; FAS, focal aware seizures; FBTCS, focal-to-bilateral tonic-clonic seizure; LTN, left temporal neocortex; RTN, right temporal neocortex; LH, left hippocampus; RH, right hippocampus. G, gliosis; NL, neuronalloss; ND, neuronal degeneration; WB, western blot; IHC, immunohistochemistry; IF, immunofluoresence; EP, electrophysiological recording.

Table 2
Information about control hippocampus.

Subjects	Gender	Age (year)	Cause of death	PMI (h)	Pathology	Seizure	Application used
1	M	43	Splenic rupture	3.5	Normal	None	IHC
2	F	41	Hemopneumothorax	4.0	Normal	None	IHC
3	M	21	Aortoclasia	4.5	Normal	None	IHC
4	F	22	Aortoclasia	2.7	Normal	None	IHC
5	M	32	Splenic rupture	3.4	Normal	None	IHC

M, male; F, female; PMI, post-mortem interval (interval between death of a patient and removal of the brain before freezing or fixation); IHC, immunohistochemistry.

Cs-Acetate (125), CsCl (10), HEPES (10), EGTA (5), TEA-Cl (5), ATP-Mg (5), 280−290 mOsm, pH 7.3 adjusted by CsOH. For sIPSC recording in the CA1 pyramidal neurons, intracellular solution contained (in mM); $CsMeSO_3$ (130), NaCl (10), EGTA (10), $CaCl_2$ (1), HEPES (10) and ATP-Mg (2). Recordings were obtained at a membrane potential of -10 mV near the reversal potential of glutamate EPSCs according to the methods established in a previous study. [15] Slices were transferred to a recording chamber and continuously perfused (2 ml/min) with oxygenated ACSF.

Drugs were applied via the perfusion system. Patch pipettes were pulled at a resistance of 3-6 MΩ for recording. All recordings were performed by a HEKA EPC10 amplifier at room temperature. Signals were low-pass filtered at 2 kHz and digitized at 5 kHz. A similar number of neurons was collected from multiple slices per specimen to ensure the independence of statistical data collected from multiple specimens. Cells were excluded from the analysis if the series resistance increased by >15% during recording or exceeded 20 MΩ. Data were analyzed offline (clampfit 10, Mini analysis) and plotted in the Origin 8 graphing software.

2.4. MQAE fluorescence detection

Brain slices were labeled in oxygenated ACSF containing 5 mM chloride indicator MQAE (N- [Ethoxycarbonylmethyl] -6- methoxyquinolinium bromide) (Invitrogen, E3101) for 40-45 min at room temperature, and transferred to a perfusion chamber (2 ml/min) for 30 min to wash out extracellular MQAE. MQAE fluorescence intensity was measured using a Leica SP5 confocal laser scanning microscope (Leica, Nussloch, Germany) tuned to 350 nm.

2.5. Seizure study with TLE mice

Mice were randomly assigned to control and experimental groups according to a computer generated sequence. In the experimental group, mice received right intrahippocampal kainic acid (KA) injection (200 ng, AP: -1.8 mm, ML: +1.8 mm, DV: +2.0 mm) on a stereotaxic frame under anesthesia with isoflurane (1-2%) according to previous methods. [16,17] The injection was performed using a thin glass capillary tube of 50-100 μm diameter at the tip with a Hamilton syringe over 5-10 min. Acute seizure attack was stopped by diazepam (10 mg/kg, i.p.) two hours after KA injection. Animals were taken supportive care after the injection to increase the survival rate. Mice were excluded from the study if they did not develop spontaneous chronic seizure discharge two months after KA injection. Age- and weight-matched control mice received PBS injection.

2.6. Electrode implantation

The implantation in mice was performed according to the coordinates in the brain atlas. Mice were anesthetized with isoflurane (1-2%) and placed in a stereotaxic frame. Recording electrodes were implanted after the chronic status epilepticus was established: two fixed recording microelectrodes (tungsten wire, 60 μm in diameter) in the bilateral hippocampal CA3 region (AP: -1.94 mm, ML: 1.9 mm, DV: 1.9 mm), two steel screws on bilateral frontal lobe (AP: +1.0 mm, ML: 2.0 mm), one steel screw on contralateral occipital lobe (AP: -4.0 mm, ML: 4.0 mm) as “reference” electrode and one olfactory “grounded” electrode (AP: +4.1 mm, ML: 1.0 mm). The entire implant was insulated using dental acrylic for long term EEG recordings. Animals were allowed to recover from surgery for at least 48 hours before recording.

2.7. EEG recording and analysis

EEG data in animals was low-pass filtered at 500 Hz, sampled at 3 kHz and saved digitally using DataWave Sciworks software (Parsippany, NJ). Electrographic seizures were identified by their characteristic pattern of discrete periods of rhythmic spike discharges, which

evolved in frequency and amplitude lasting at least 10 seconds and ended with repetitive burst discharges and voltage suppression. Ictal HFOs were detected by band-pass filtration of the recordings at 80-500 Hz. To be considered as a HFO candidate, oscillatory events in the frequency range had to show at least four consecutive cycles with an amplitude of three standard deviations (SD) above the mean of the reference period. The detected HFOs were then extracted and used for further analysis. The time frequency analysis was performed using Z-scored wavelet transform procedures to present relative changes in magnitude. Warmer color represents greater Z-scores. The Fourier transformation was used for power spectrum analysis. For each animal, EEG was recorded in the home cage with access to food and water for continuous twenty-four hours, and the number of seizures per four hours was obtained by dividing the total number of seizures by the total number of recording hours and multiplied by four.

For TLE patients, depth electrodes (0.8 mm diameter, 16 contacts of 2.0 mm length, spacing between contacts centres 1.5 mm, SDE-08, HKHS, China) were implanted stereotactically into the targeted areas. Electrode locations were identified by coregistering a postimplantation CT image to a preimplantation T1-weighted MRI, which was then normalized to MNI space in SPM12. To assign a label of cortical and subcortical regions to each electrode, we segmented each patient's structural MRI using FreeSurfer 7.1 and Fieldtrip. [18,19] The anatomical locations of each electrode were visually verified by two experienced neurosurgeons. EEG data in TLE patients were collected by the EEG-1200C (NIHON KOHDEN, Japan) at 2 kHz, and low-pass filtered at 600 Hz. A bipolar montage was used to record and review the EEG data. HFOs in patients were detected and counted by an automated detector similar to a previously established procedure with slight modification. [20] The number of HFOs per seizure in TLE patients was calculated as the average of HFOs in three seizure attacks and reviewed by two experienced electrophysiological experts. The time-frequency and power of HFOs analyses were performed in the same procedure as in rodents. All analyses were performed by at least two investigators who were blinded to experimental groups according to previous studies. [21]

2.8. Immunostaining

Paraffin-embedded tissues were sectioned at 6 μm. Sections were heated 20 min for antigen retrieval after deparaffinization and rehydration. Endogenous peroxidase activity was blocked with 3% H_2O_2. After blocking with bovine serum, sections were incubated with the rabbit anti-ClC-3 antibody (Alomone Labs Cat# ACL-001, RRID: AB_2039814) overnight at 4°C. Sections were then incubated with goat anti-rabbit immunoglobulin conjugated to peroxidase-labeled dextran polymer for one hour at 37°C after being washed with PBS three times, and DAB (3,3'-diaminobenzidine) subsequently for appropriate time according to manufacturing instructions. Counterstaining was performed with hematoxylin. To evaluate the immunoreactivity of ClC-3, three sections from each specimen were selected and three visions were captured (200 × or 400 × magnification, resolution 4080 × 3027) in each section, and the optical density (OD) was evaluated with imageJ and IHC profiler plugin according to a previous method. [22] The average OD of the three sections was determined as the OD of ClC-3 in the specimen. All images were taken with an upright bright-field microscope (BX63, OLYPUS, Japan).

For double immunofluorescence staining, samples from mice with chronic TLE were cryoprotected in 30% sucrose solution at 4°C for 48 h after fixation. The tissues were sectioned at 25 μm thickness using a cryostat microtome. Frozen sections from TLE mice or paraffin sections from TLE patients were incubated with the rabbit anti-ClC-3 (Alomone Labs Cat# ACL-001, RRID: AB_2039814) and mouse anti-NeuN antibodies (Millipore Cat# MAB377, RRID: AB_2298772) overnight at 4°C after blocking with bovine serum. After washing three times with PBS, sections were incubated with Alexa Fluor 555-conjugated goat anti-rabbit IgG (Thermo Fisher Scientific Cat# A-21428, RRID: AB_2535849) and Alexa Fluor 488-conjugated donkey anti-mouse IgG (Thermo Fisher Scientific Cat# A-21202, RRID: AB_141607) secondary antibodies for one hour at room temperature and washing with PBS three times. All images were taken with an inverted laser scanning confocal microscope equipped with a Zeiss GaAsP Airyscan detection connected to the Zen 2.3 system (LSM800; Zeiss; Germany).

2.9. Western blot

Total proteins were extracted from the hippocampus of chronic TLE and control mice using a total protein extraction kit according to manufacturing instructions (Beyotime Biotechnology, Shanghai, China). Equal amounts of protein (60 ug/lane) were separated on the SDS-Polyacrylamide Bis-Tris 10% gels and transferred to polyvinylidene difluoride (PVDF) membranes. The membranes were blocked by 5% BSA at room temperature for one hour and incubated with the rabbit anti-ClC-3 (Alomone Labs Cat# ACL-001, RRID: AB_2039814) and rabbit anti-GAPDH (Sigma-Aldrich Cat# G9545, RRID: AB_796208) antibodies overnight at 4°C. After washed with TBST three times, the membranes were incubated with horseradish peroxidase (HRP)-conjugated secondary antibody (Beyotime Biotechnology, Shanghai, China) at room temperature for one hour and washed with TBST three times. The immunoreactive bands were scanned after visualization using enhanced chemiluminescence and analyzed with Quantity One software. GAPDH was used as the internal control for normalization.

2.10. Ethical statements

The study was approved by the Ethics Committee of Army Medical University. The use of human samples was approved by the Ethics Committee guidelines of Army Medical University in consistent with the ethical standards in Helsinki declaration. [12] All patients or individuals involved had signed an informed consent form prior to the study. The protocol for animal experiments was carried out in accordance with the institutional animal welfare guidelines and followed the ARRIVE guidelines for reporting animal research. All the animal experimental procedures were reviewed and approved by the Internal Animal Care and Use Committee of the Army Medical University.

2.11. Statistical analysis

The proper sample size and associated study power were estimated according to the previously established experimental settings. [23] G*Power 3 was used to calculate the statistical power. For each experiment, the sample size was estimated for an effect size of 50% to 70% using the SD calculated from the control population with a power of 0.8 (β = 0.2) and an α of 0.05. The sample of each experiment was n ≥ 3. For example, in Figure 5c (Quantification of the ClC-3 protein in the homogenate of hippocampal lesions), using unpaired two-tailed t-test, six mice in each group would be sufficient to reach significance with a power of 0.9 and an α of 0.05 for the presented data.

Data acquisition and analysis were done blindly and presented as means ± SEM. Statistical methods, the number of replicates and number of animals or specimens were indicated as needed. For comparisons between two or more groups, t-test, paired non-parametric Wilcoxon rank test or two-way ANOVA followed by post-hoc analysis were used. For the comparison of the interevent interval and amplitude distribution of sIPSC in single cell, Kolmogorov-Smirnov (K-S) test was used. Spearman's rank correlation analysis was used in correlation analyses. Normality and equal variance tests were performed for all statistical analyses. Data were plotted and analyzed by Graphpad Prism 5 and Origin 8. $P < 0.05$ was considered statistically

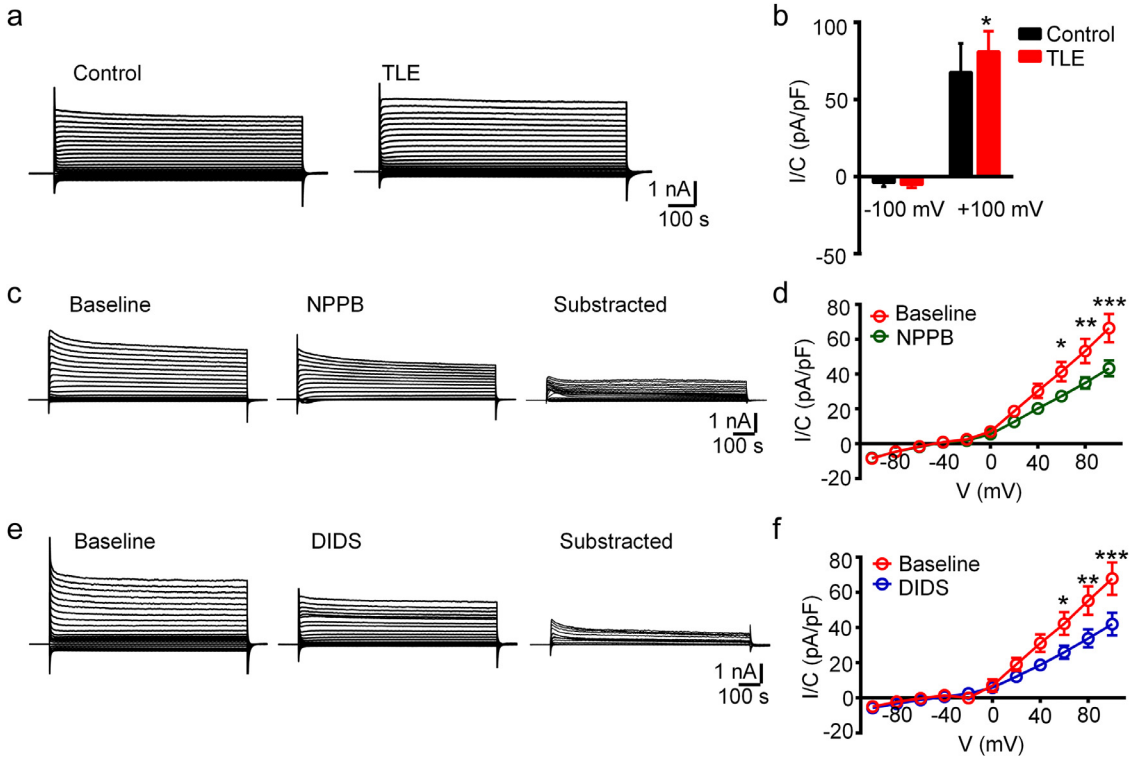

Figure 1. ClC-mediated current was increased in the hippocampal neurons of chronic TLE mice.

(a) Representative traces of ClC-mediated neuronal chloride current in the CA1 region of control and TLE mice. (b) The peak amplitude of chloride currents at +100 mV stimulation was increased in the hippocampal neurons of chronic TLE mice (*$P < 0.05$, unpaired two-tailed t-test. n = 11 neurons from total 3-4 mice for each group). (c-f) Representative traces and I-V curves showing that chloride currents induced by stepped-voltage stimulation was inhibited by NPPB or DIDS treatment (*$P < 0.05$, **$P < 0.01$ and ***$P < 0.001$, two-way ANOVA test followed by post-hoc analysis. n = 11, 13 neurons from total four mice for each group).

significant. The schematic diagram of the experimental design, the number of mice and clinical specimens and the statistical plan used in different experimental procedures were illustrated in Supplementary Figure 1.

2.12. Role of funding source

This study was supported by the National Natural Science Foundation of China (No. 81601143, No. 81771217).

3. Results

3.1. ClC-mediated current was increased in the hippocampal pyramidal neurons of chronic TLE mice

As ClC transport chloride across the plasma membrane along the electrochemical gradient, we first compared the amplitude of ClC-mediated current in neurons at the CA1 region of control and TLE mice. As shown in representative traces (Figure 1a), an outwardly rectified current was recorded in the neuron with the stepped voltage stimulation, and the statistical analysis revealed that the peak chloride current at +100 mV stimulation was increased in the hippocampal neurons of TLE group than that in control tissues ($P < 0.05$, unpaired two-tailed t-test, Figure 1b).

Next, we asked whether manipulating of ClC has any effect on the chloride current in the ipsilateral hippocampal neurons of TLE mice. To this end, we utilized NPPB and DIDS, two broad-spectrum blockers for chloride channels with demonstrated function in regulating voltage-gated chloride currents in glioma cells or cultured neurons. [14,24,25] As shown in representative traces and subtracted traces (Figure 1c, e), the chloride current we recorded was sensitive to NPPB or DIDS treatment. The current-voltage curves of the steady-state current showed that the density of ClC-mediated current at +60, +80 and +100 mV stimulation was significantly reduced by the drug treatment ($P < 0.05$, $P < 0.01$ and $P < 0.001$, respectively, two-way ANOVA test followed by post-hoc analysis, Figure 1d, f). Together, these data indicated that ClC are significantly involved in mediating neuronal chloride current under the epilepsy context.

3.2. The inhibitory synaptic transmission in hippocampal neurons of chronic TLE mice was increased by NPPB and DIDS

As NPPB and DIDS both inhibited ClC-mediated outward chloride current in the hippocampal neurons of TLE mice and inhibitory synaptic transmission in neurons is mainly mediated by chloride influxes, we next investigated the effects of NPPB and DIDS on the spontaneous IPSC (sIPSC) in the CA1 pyramidal neurons of chronic TLE mice. To ensure that the currents recorded at -10 mV in cesium-based intracellular solution were pure sIPSC, we compared the sIPSCs frequency and amplitude before and after the treatment of glutamatergic blockers CNQX and AP-5. Both representative traces and statistical analyses showed that the frequency and amplitude of sIPSC events were similar before and after the CNQX/AP-5 treatment (Supplementary Figure 2a, b). As the chloride influxes were mainly mediated by $GABA_A$ receptors, we additionally applied bicuculline (a $GABA_A$ receptor blocker) and strychnine (a glycine receptor blocker) sequentially at the end of sIPSC recording. The results showed that the sIPSC events were blocked by bicuculline and strychnine (Supplementary Figure 2c), suggesting the outward currents recorded were mostly sIPSC. Subsequently, we evaluated the effects of NPPB and DIDS on sIPSC in the CA1 pyramidal neurons in chronic TLE mice. As shown in representative recording traces (Figure 2a, b), an outward current was induced after NPPB or DIDS treatment in the recorded cells. We measured the amplitude of the outward current by subtracting the steady-state value (set as baseline) from the peak value observed at approximately 5 min after drug treatment in all the

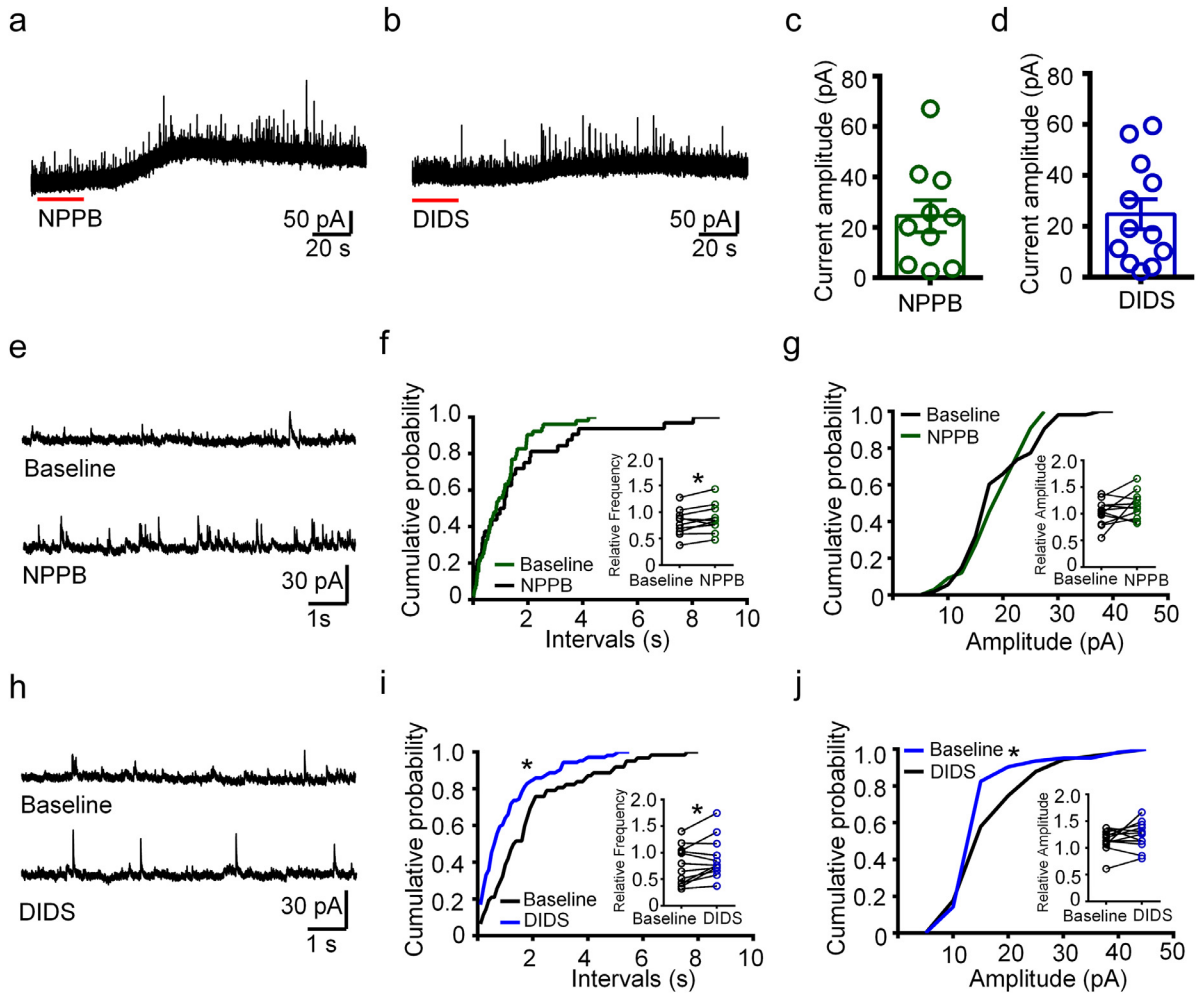

Figure 2. The inhibitory synaptic transmission was increased by NPPB or DIDS in hippocampal neurons of TLE mice.

(a, b) Representative traces of sIPSC recorded with NPPB or DIDS treatment in hippocampal neurons of TLE mice. (c, d) Scatter-bar plots showing the amplitude of the outward currents after NPPB or DIDS treatment in the recorded cells. n = 10 (c) and 12 (d) neurons from total five mice. (e) Representative traces of sIPSC recorded in the pyramidal neuron shown in (a) before ("Baseline") and after NPPB treatment. (f, g) Cumulative probability curves showing that neither inter-event interval or amplitude of sIPSC was affected by NPPB in the cell presented in (a). ($P > 0.05$, K-S test). Inset: the relative frequency of sIPSC was increased by NPPB treatment, while the relative amplitude was not affected. (*$P < 0.05$, paired two-tailed t-test, n = 10 neurons from total five mice). (h) Representative traces of sIPSC recorded in the pyramidal neuron shown in (b) before ("Baseline") and after DIDS treatment. (i, j) Cumulative probability curves showing that the increased inter-event interval and amplitude of sIPSC in the cell presented in (b) after DIDS treatment. (*$P < 0.05$, K-S test). Inset: the relative frequency of sIPSC was increased by DIDS treatment, while the relative amplitude was not affected. (*$P < 0.05$, paired two-tailed t-test, n = 12 neurons from total five mice).

recorded cells (Figure 2c, d). We analyzed the cumulative probability of inter-event intervals and amplitude of sIPSC before and after NPPB treatment. While the sIPSC frequency was increased ($P < 0.05$, paired two-tailed t-test, Figure 2e, f), the amplitude was not affected (Figure 2g). Similarly for DIDS, statistical analysis revealed that the sIPSC frequency was increased after the treatment ($P < 0.05$, paired two-tailed t-test, Figure 2h, i), whereas the sIPSC amplitude was not affected (Figure 2j). Taken together, these results suggest that NPPB or DIDS treatment increases inhibitory synaptic transmission in the pyramidal neurons in CA1 region of chronic TLE mice.

3.3. NPPB and DIDS ameliorated the seizure activity in mice with chronic TLE

Next, we investigated whether *in vivo* administration of NPPB and DIDS could alleviate seizure activity in mice with chronic TLE. We first sought to generate the chronic epilepsy mouse model to mimic the electroencephalography, histopathology and synaptic reorganization of TLE in patients [16,17]. To this end, we performed an intrahippocampal injection of 200 ng KA to the experimental mice, which were followed by approximately two months to develop stable chronic epileptic activity. [26] Chronic status epilepticus was successfully recorded in these mice, as evidenced by the observations that seizure initiated at the ipsilateral hippocampus, propagated to contralateral hippocampus and ipsilateral frontal lobe gradually (Figure 3a).

To test the effects of NPPB and DIDS on chronic seizure activity in the mouse model, we set the dose of the drug to be 20 mg/kg (i.p.), since this dose was previously reported to efficiently modulate pain threshold in animals with chronic pain. [27] NPPB or DIDS was administrated once a day without any observable side effects, and EEG was recorded simultaneously. Statistical analysis showed that the number of spontaneous status epilepticus in 0-4 hours after NPPB or DIDS injection was reduced compared to the number of seizures per 4 hours in the remaining 4-24 hours (set as baseline) respectively (Figure 3b, c) (b, $P < 0.001$, paired non-parametric Wilcoxon rank test. c, $P < 0.01$, paired non-parametric Wilcoxon rank test). However, the duration of each status epilepticus was not affected in 0-4 hours after NPPB or DIDS injection (Figure 3d, e). We speculated that the neuronal network in chronic status epilepticus is complicated, and seizure duration can be affected by many factors but not NPPB or DIDS alone.

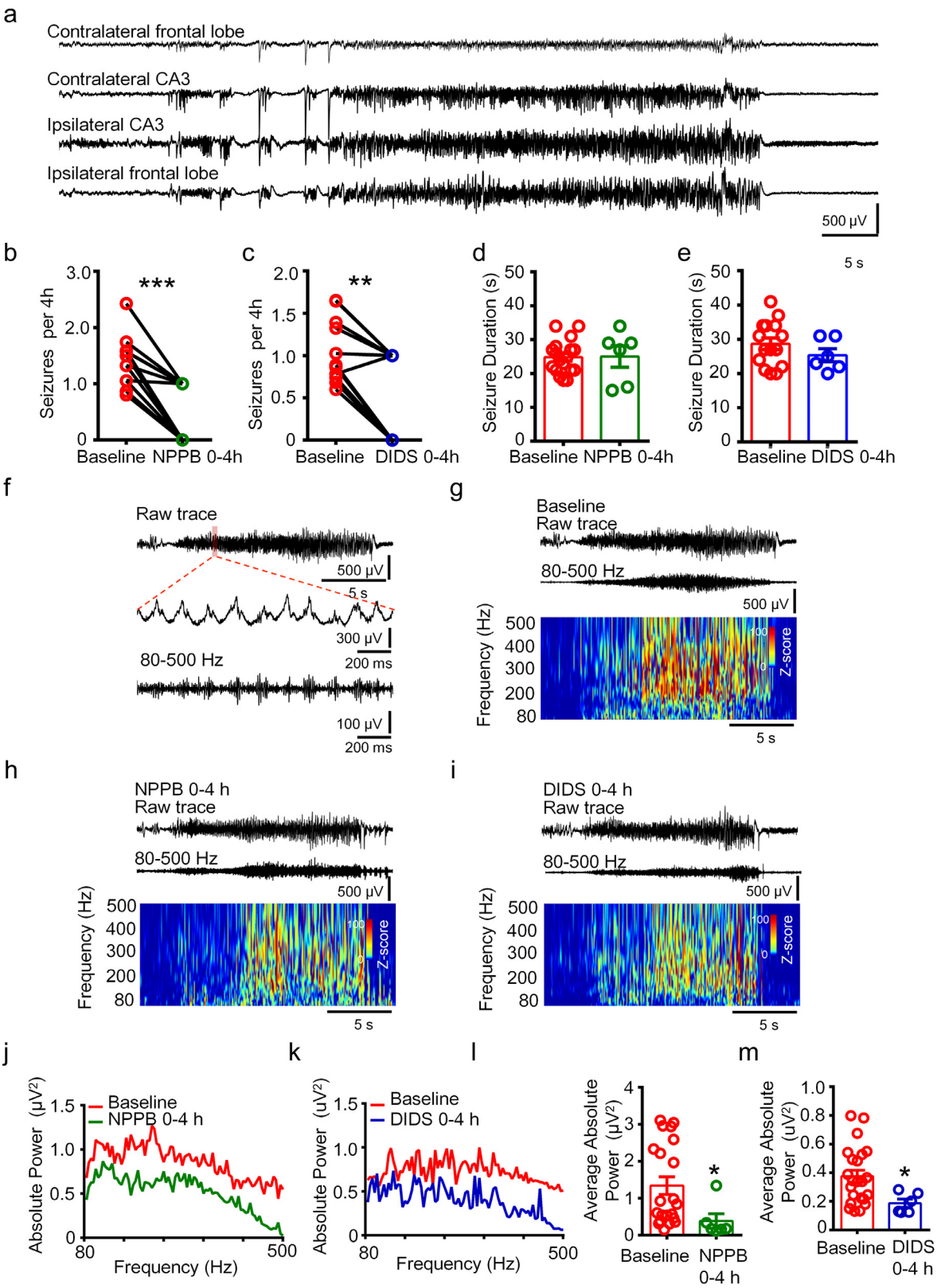

Figure 3. NPPB and DIDS ameliorated seizure activity in the chronic TLE mice.

(a) Representative raw traces of recorded status epilepticus in multiple encephalic sites of the chronic TLE mice. (b, c) The number of seizure discharges was reduced in 0-4 hours after NPPB or DIDS injection (***$P < 0.001$, **$P < 0.01$, paired non-parametric Wilcoxon rank test, n = 12, 11 mice for each group). (d, e) The duration of each status epilepticus was not altered by NPPB or DIDS injection ($P > 0.05$, unpaired two-tailed t-test. n = 6-18 seizures from total six mice in each group). (f) Representative raw trace of status epilepticus recorded in the ipsilateral hippocampus of the chronic TLE mice. HFOs (80-500 Hz) were obtained after band-pass filtration of the raw trace. (g-i) Relevant time-frequency analysis of the band-pass filtered HFOs (80-500 Hz) recorded in the ipsilateral hippocampus of TLE mice before and after NPPB or DIDS injection. (j, k) Power spectrum traces showing the distribution of the absolute power of HFOs at 80-500 Hz in the ipsilateral hippocampus in 0-4 hours and 4-24 hours (set as baseline) after NPPB or DIDS treatment. (l, m) The average absolute power of ictal HFOs at 80-500 Hz in the ipsilateral CA3 region was reduced in 0-4 h after NPPB or DIDS treatment. (*$P < 0.05$, unpaired two-tailed t-test, n = 6-18 seizures from total six mice for each group).

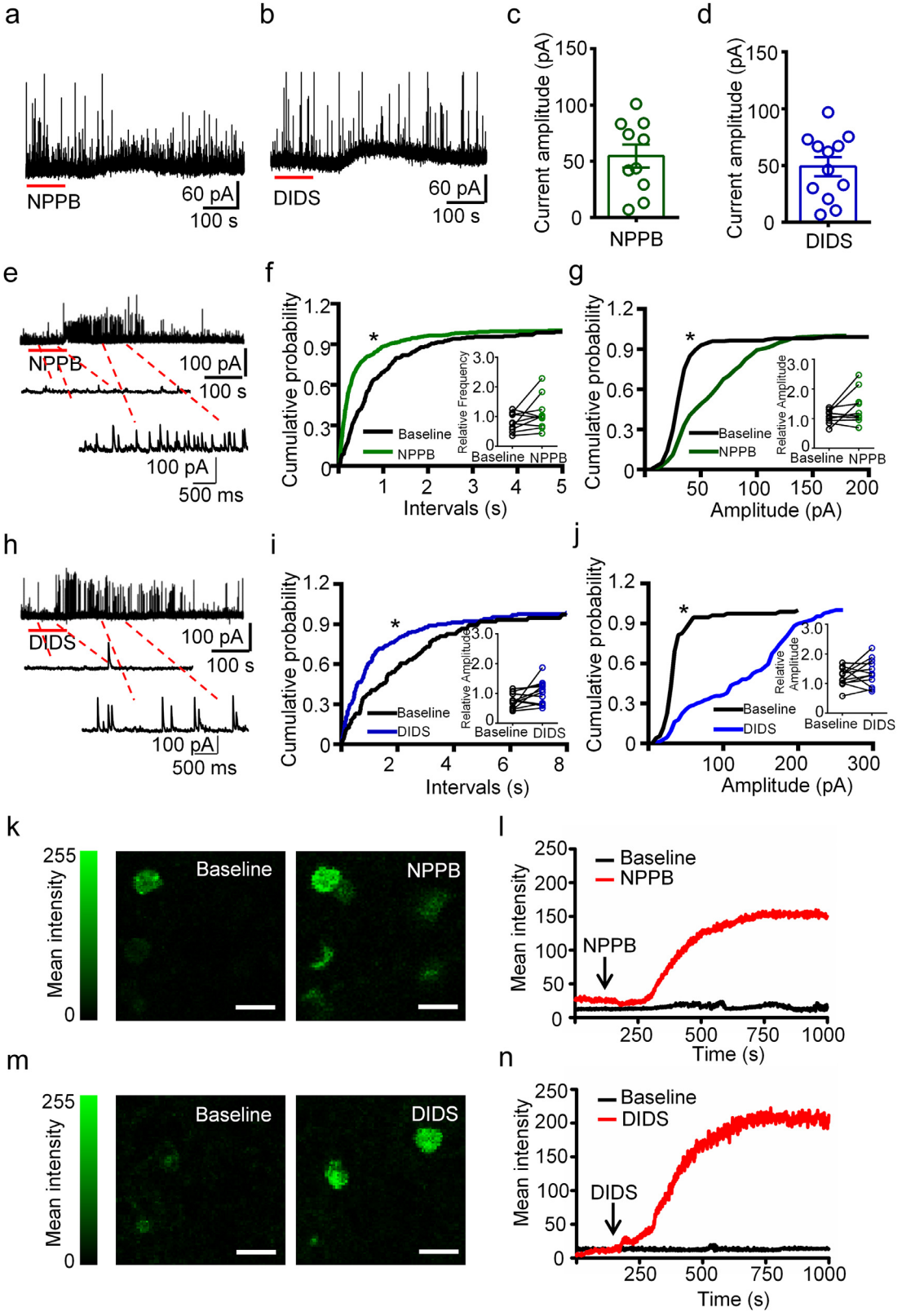

Figure 4. NPPB and DIDS induced outward currents in hippocampal neurons of intractable TLE patients.

(a, b) Representative traces of sIPSC showing outward currents after NPPB or DIDS treatment in the hippocampal neurons of intractable TLE patients. (c, d) Scatter-bar diagram showing the amplitude of the outward currents induced by NPPB or DIDS in recorded cells. n = 10 (c) or 12 (d) neurons from total six specimens for each group. (e) Representative traces of sIPSC showing robust increase of frequency and amplitude of sIPSC in responding to NPPB treatment. (f, g) Cumulative probability curves showing increased inter-event interval and amplitude of sIPSC after NPPB treatment in the cell presented in (e) (***$P < 0.001$, K-S test). Inset: the relative inter-event interval and amplitude were not significantly affected by NPPB in the hippocampal neurons of TLE patients. ($P > 0.05$, paired two-tailed t-test, n = 10 neurons from total six specimens). (h) Representative traces showing increased sIPSC frequency and amplitude in responding to DIDS treatment. (i, j) Cumulative probability curves showing increased inter-event interval and amplitude of sIPSC in the cell presented in (h) after DIDS treatment (***$P < 0.001$, K-S test). Inset: the relative inter-event interval and amplitude of sIPSC were slightly increased after DIDS treatment ($P >$ 0.05, paired two-tailed t-test, n = 12 neurons from total six specimens). (k, l) Representative images and real-time intensity curves showing increased immunofluorescence intensity

High-frequency oscillations (HFOs) are mainly generated by pyramidal cells in response to GABA released from interneurons and reflect population spike bursts arising from synchronized discharges of abnormally bursting principal cells and interneurons. [28,29] HFOs occur in the EEG recordings of TLE patients and animal models, and have been used as an electrophysiological biomarker in epilepsy. [30-33] Thus, we wondered whether the HFOs in the hippocampus of TLE mice would be affected by modulating the intracellular chloride homeostasis with NPPB or DIDS. HFOs are generally analyzed above 80 Hz, while the upper-limit for recording might vary. Oscillations between 80 and 200 Hz (ripples) are found in humans and correlate with the severity of local atrophy in TLE patients, oscillations between 250 and 500 Hz (fast ripples) are identified in epileptogenic areas and represent the hypersynchronous discharging of locally interconnected principal neurons and interneurons capable of generating spontaneous seizures. [34-36] In our study, we analyzed the HFOs at the scope of 80-500 Hz. In status epilepticus activity recorded from the ipsilateral hippocampus, ictal HFOs were obtained after band-passed filtration of the raw traces and concomitantly generated in the spike activity generally (Figure 3f), which is consistent with previous studies. [35,37] We analyzed the time-frequency diagram of ictal HFOs recorded in 0-4 hours after NPPB or DIDS injection, as shown in the representative traces and corresponding time-frequency diagrams (Figure 3g-i). The magnitude of HFOs in baseline was slightly higher (warmer color represents greater Z-score). We analyzed the distribution of ictal HFOs between 80 and 500 Hz in NPPB or DIDS treated mice (Figure 3j, k) and found that the average absolute power of ictal HFOs at this range was reduced in the seizure activities that occurred in 0-4 hours after the drug treatment ($P < 0.05$, unpaired two-tailed t-test, Figure 3l, m). Taken together, these results suggest that NPPB and DIDS ameliorate the seizure severity *in vivo* in chronic TLE mice.

3.4. NPPB and DIDS induced outward currents in neurons of CA1 region in TLE patients

We next sought to verify the effects of NPPB and DIDS on the inhibitory synaptic transmission in CA1 pyramidal neurons of sclerotic hippocampus of TLE patients. Slices from six patient sclerotic hippocampi were used in our study (Table 1). Consistent with the observation from TLE mice, application of NPPB and DIDS induced outward currents in eight out of ten and ten out of twelve recorded neurons, respectively, as shown by representative traces and the measurement of the amplitude of outward currents (Figure 4a-d). Additionally, we observed two recorded cells in each group responding to the NPPB or DIDS treatment with weak outward current but significant increase of sIPSC frequency and amplitude (Figure 4e-j) ($P < 0.05$, K-S test). Interestingly, statistical analysis showed that the inter-event interval and amplitude of sIPSC were not significantly affected by NPPB or DIDS in all the recorded hippocampal neurons of TLE patients (Insets in Figure 4e-j) ($P > 0.05$, paired two-tailed t-test), which might attribute to the heterogeneity of human hippocampus when compared with the hippocampus from experimental mice. Because human hippocampus samples were collected from patients with different ages, different seizure duration or have taken different AEDs before surgery, whereas the hippocampus dissected from experimental mice were less various because they were sustained with similar treatment at a similar age and housed under the same condition.

Furthermore, we monitored the effect of NPPB and DIDS on intracellular chloride concentration ($[Cl^-]_i$) in slices sectioned from the hippocampus of TLE patients using MQAE (N-Ethoxycarbonylmethyl -6- methoxyquinolinium bromide), a chloride indicator that would be quenched via collision with increased intercellular chloride. Fluorescent images and the plotted real-time density curves showed that the mean fluorescence intensity of MQAE was increased remarkably after NPPB or DIDS treatment, suggesting that the $[Cl^-]_i$ in the detected cells were decreased, ultimately leading to the increase of the transmembrane chloride electrochemical gradient (Figure 4k-n). Taken together, these results suggest that NPPB and DIDS induce outward currents in CA1 pyramidal neurons of TLE patients by increasing the transmembrane chloride electrochemical gradient.

3.5. The expression of ClC-3 was increased in the hippocampus of mice with chronic TLE

Next, we investigated whether the expression of ClC components were altered in the ipsilateral hippocampus of mice with chronic TLE. We focused on *ClC-3*, the major ClC gene family member with known expression in the brain and its possible roles in tonic-clonic seizures. [8,9] We picked the first section in every five continuous frozen sections (25 μm) of the hippocampus (from anterior to posterior) and performed double immunofluorescence staining. In our samples, ClC-3 was expressed in the NeuN positive hippocampal neurons in CA1 region of both control and TLE mice (Figure 5a). The expression pattern of ClC-3 in the CA1 region was similar between the anterior and posterior hippocampus (Data not shown). In addition, western blot detected the ClC-3 immunoreactive bands at approximately 87 kDa in gel electrophoresis (Figure 5b), which is consistent with previous studies. [38] Quantitative analysis revealed that the protein expression of ClC-3 was increased in the hippocampus of chronic TLE mice (Figure 5c) ($P < 0.01$, unpaired two-tailed t-test).

We further analyzed the correlation between the expression of *ClC-3* (relative optical density, OD) and various epileptical characterizations of the chronic TLE mice, including the number of seizures per day, average seizure duration, and average absolute power of ictal HFOs. Spearman's rank correlation analysis showed that the expression of *ClC-3* was positively correlated with the average absolute power of ictal HFOs in TLE mice ($P < 0.05$), but not with the number of seizures per day and average seizure duration ($P > 0.05$) (Figure 5d-f).

3.6. Correlation between ClC-3 protein level and clinical characteristics in TLE patients

Finally, we assessed the expression of *ClC-3* in the hippocampus of intractable TLE patients (Table 1) and age-matched donors (Table 2). Immunohistochemical staining found that ClC-3 was expressed in the neurons of CA1 region in the control and sclerotic hippocampus (Figure 6a). Mean density of the immunoreactivity of ClC-3 was reviewed according to previous methods, [22] and the results showed that the intensity of ClC-3 immunoreactivity was increased in the CA1 region of TLE patients (Figure 6b) ($P < 0.05$, unpaired two-tailed t-test). Double immunostaining additionally revealed that ClC-3 was co-expressed with NeuN in the CA1 region of the hippocampus in TLE patients (Figure 6c).

Depth electrodes were implanted in the targeted brain area of TLE patients to locate the onset zone of seizure. Propagated seizure activity was recorded in multiple sites by the recording montage in a representative TLE patient (Supplementary Figure 3). The depth electrode targeted the left hippocampus in the representative TLE patient was shown (Figure 6d). Seizure activity in the CA1 region of the hippocampus was recorded by the indicated bipolar contacts (arrows in Figure 6d), and ictal HFOs were obtained after filtration of

of intracellular chloride indicator MQAE after NPPB treatment in the hippocampal neurons. (n = 3 slices respectively from total three specimens). (m, n) Representative images and real-time intensity curves showing increased immunofluorescence intensity of intracellular chloride indicator MQAE after DIDS treatment in the hippocampal neurons. (n = 4 slices respectively from total three specimens).

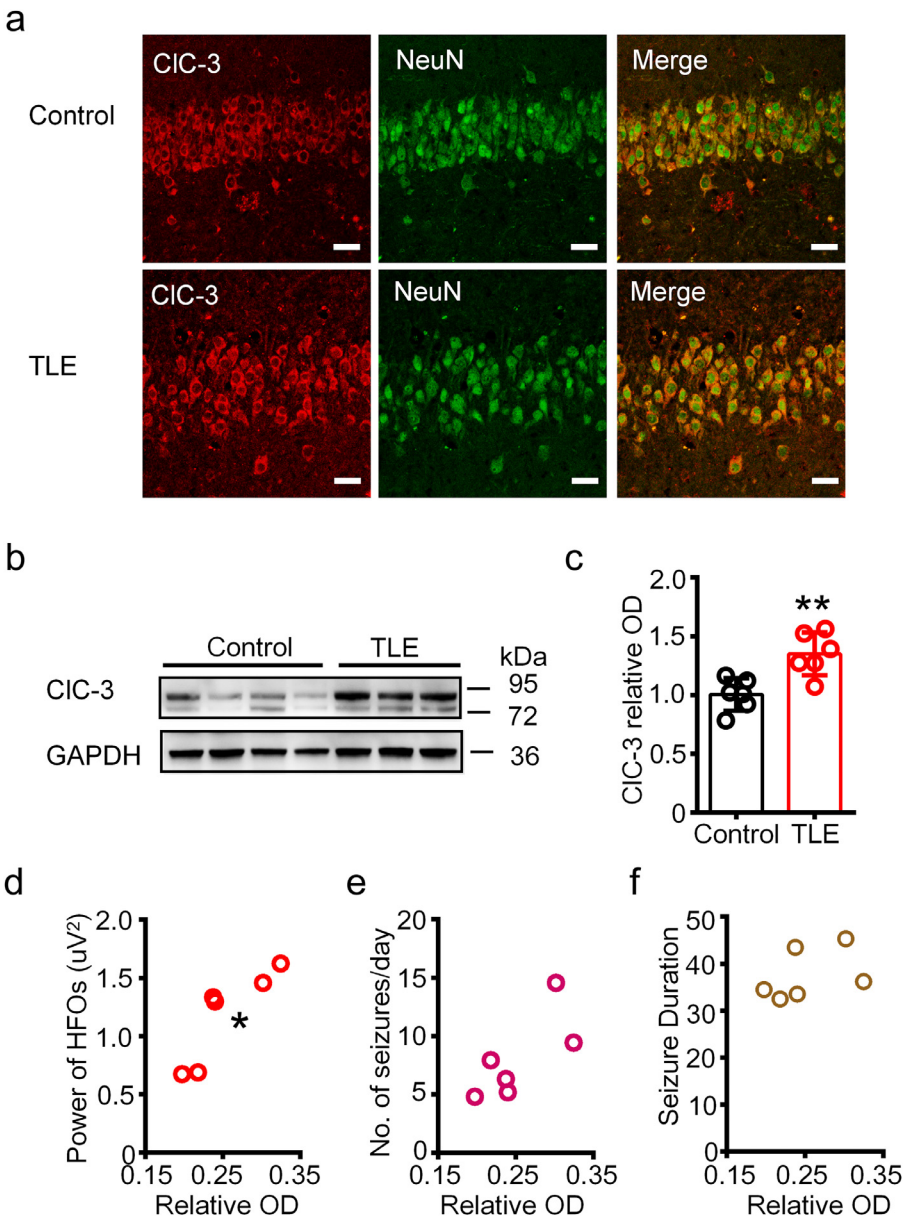

Figure 5. The expression of ClC-3 was increased in the ipsilateral hippocampus of chronic TLE mice.

(a) Representative double immunofluorescence images showing the neuronal co-expression of ClC-3 and NeuN in the hippocampal CA1 region of control and chronic TLE mice. Scale bar, 20 μm. Images were selected from three mice for each group. (b) The ClC-3 protein in the homogenates of hippocampus from control and TLE mice was detected at 72-95 kDa by Western blot. (c) Densitometric analysis results showing the increased expression of ClC-3 in the hippocampus of the chronic TLE mice. (**$P < 0.05$, unpaired two-tailed t-test, n = 6 mice for each group). (d-f) Spearman's rank correlation between the expression of ClC-3 in the hippocampus and the average absolute power of ictal HFOs (d, rho = 0.9429, *$P < 0.05$), the number of seizures per day (e, rho = 0.7409, $P > 0.05$) and average seizure duration (f, rho = 0.4857, $P > 0.05$). n = 6 mice for each analysis.

the raw traces, as shown by the temporal traces and the illustration of the single burst-like HFO (Figure 6e). Time-frequency diagram indicated that the oscillations between 80-250 Hz were the primary band of HFOs in the hippocampus of the TLE patient (Figure 6e). We assessed the correlations between the protein level of ClC-3 in the CA1 region of the sclerotic hippocampus and relevant clinical characteristics in all the fifteen TLE patients. The expression of ClC-3 was positively correlated with the number of ictal HFOs per seizure in the hippocampus of TLE patients (Figure 6f) ($P < 0.05$, Spearman's rank test), but not with the absolute power of HFOs per seizure, course of epilepsy, seizure frequency per month or categories of AEDs taken (Figure 6g-j). Together, our results from mice and TLE patients suggest that ClC-3 encodes the important ClC component mediating the neuronal chloride current homeostasis and its expressional alteration might account for the aberrant electrophysiological activities in TLE.

4. Discussion

Here, we combined mouse models and patient specimens and provided evidence that ClC were involved in mediating various electrophysiological activities of TLE. We utilized ClC inhibitors to show that targeting ClC might be an effective therapeutical strategy to ameliorate seizures. Moreover, our expressional characterization followed by correlation analysis suggested that ClC-3 might encode the important ClC component accounting for the increase of ClC-mediated current in hippocampal lesions and therefore deserve further investigation for more precise TLE targeting.

Our study first characterized the pathogenic function of ClC in hippocampal neurons. In mature neurons, the intracellular chloride is maintained at a very low level under normal physiological conditions for maintaining the resting membrane potential. Previously studies

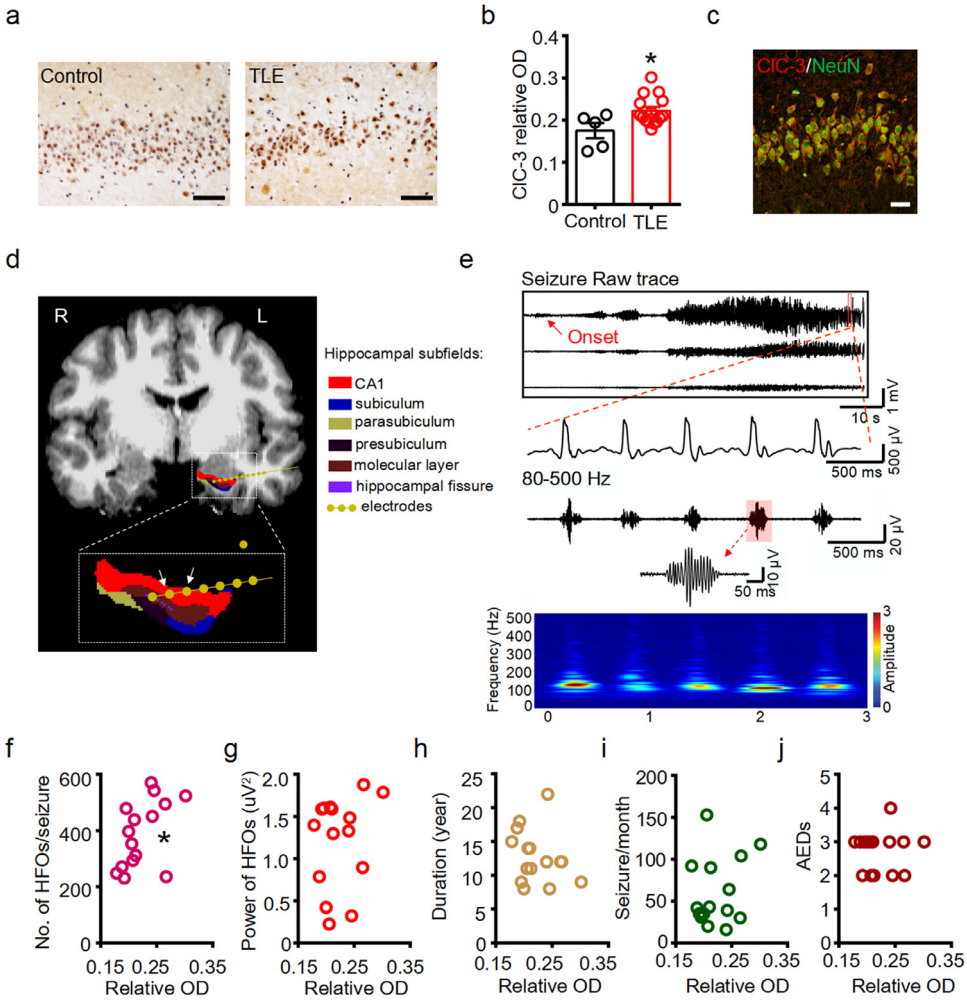

Figure 6. The expression of ClC-3 in the CA1 region was positively correlated with the number of HFOs per seizure in TLE patients.

(a) Representative immunohistochemical images showing increased ClC-3 protein abundance in the neurons at the hippocampal CA1 region from control donors and TLE patients. Scale bar: 50 μm. (b) Scatter-bar plots showing the increased immunoreactivity of ClC-3 in the CA1 region of TLE patients (**$P < 0.01$, unpaired two-tailed t-test, n = 5, 15 specimens for each group). (c) Representative double immunofluorescent image showing the co-expression of ClC-3 and NeuN in the CA1 region of sclerotic hippocampus of TLE patients. Scale bar: 20 μm. Image was selected from three specimens. (d) Representative image showing the implantation of a depth electrode in the CA1 region of the left hippocampus in a representative TLE patient. Arrows indicates the contacts at hippocampus used for HFOs detection. (e) Representative EEG traces of a seizure activity initiated at the indicated contacts of the depth electrode showed in (d). Upper panel: raw EEG traces showing the initiation and propagation of a seizure activity; middle panel: spike activities in the seizure discharging; bottom panel: filtered HFOs at 80-500 Hz corresponding to the spike activities in the middle panel (Inset: illustration showing the oscillation cycles of a single HFO). Relative time-frequency analysis showed the recorded ictal HFOs concentrated in the band scope of 80-250 Hz. (f) Spearman's rank correlation between the expression of ClC-3 in the CA1 region and the number of ictal HFOs per seizure in the hippocampus of TLE patients (rho = 0.4883, *$P < 0.05$). n = 15 patients. (g-j) No significant correlation between ClC-3 protein level and the average power of ictal HFOs (g, rho = -0.1545, $P > 0.05$), course of epilepsy (h, rho = -0.116, $P > 0.05$), seizures per month (i, rho = -0.09502, $P > 0.05$) and categories of AEDs taken (j, rho = 0.2556, $P > 0.05$) in TLE patients. n = 15 patients for each analysis.

have identified abnormal accumulation of intracellular chloride altered the GABAergic transmission in epileptogenic foci, [39-44] factors such as the cation-chloride cotransporter *NKCC1* and the potassium-coupled chloride transporter *KCC2* are involved. [45-48] By using the chronic TLE model, we found that the outwardly rectified chloride current mediated by ClC was increased in the hippocampal neurons, suggesting that ClC might be another potential etiologic factor for intracellular chloride accumulation in the neurons of TLE hippocampal lesions.

We further showed that blocking ClC by small molecules (NPPB and DIDS) affected not only the outwardly rectified chloride, but also the inhibitory synaptic transmission in the hippocampal lesions. These observations were recapitulated in TLE patients, though the frequency and amplitude of sIPSC varied across individuals. Our chronic TLE mouse model manipulation found that administration of NPPB or DIDS ameliorated the seizure activity, suggesting that ClC are attractive drug targets for seizure treatment.

Our study also delineated the HFO profile under the ClC blockage. Previous studies have found that higher rates of HFO ripples (80-200 Hz) in the hippocampus correlate with the severity of local atrophy in TLE patients with hippocampal sclerosis. [49] Also, increased amplitude of HFOs has been identified from the pathological granule cell layer of the dentate gyrus in animals with status epilepticus. [28] The amplitude of ripples (80-250 Hz) is typically largest in the pyramidal cell layer and increasing the fidelity of pyramidal cell discharges restored the amplitude of pathological HFOs in epilepsy. [50,51] We found the average absolute power of ictal HFOs in the hippocampus of TLE mice was reduced in 0-4 hours after NPPB or DIDS administration, suggesting that the power of ictal HFOs was affected by the neuronal chloride concentration and these drugs ameliorated the intensity of status epilepticus besides reducing the seizure frequency.

Finally, we characterized the expression of the ClC gene family member, *ClC-3*, in seizure lesions and correlated the expression to

relevant electrophysiological activities. Among the constitutively activated ClC family members, *ClC-3* is one of the major isoforms expressed in the brain and was considered as the crucial ClC component in mediating the outwardly rectified chloride current. [3,6] We found that the hippocampal expression of ClC-3 was positively correlated with the average absolute power of HFOs in TLE mice and the number of ictal HFOs per seizure in TLE patients, suggesting that increased expression of ClC-3 might promote epileptogenic events via affecting HFOs. These results also indicated that targeting ClC-3 might further represent a more effective and precise TLE treatment option.

In summary, our results characterized the potential role of ClC in the eplileptogenesis of TLE by modulating the intracellular chloride concentration and emphasized the significance of electrochemical equilibrium in maintaining neuron excitability. Targeted inhibition of ClC may be a potential therapeutic strategy to ameliorate seizure activity.

5. Contributors

K.F. S. and C.Q. Z. contributed to conception and study design; K.F. S., X.L. Y., G.L. L., G. Z., Z.K. W., X.J. S., T.T. W. and Z.F. W. contributed to acquisition and analysis of data, and S.Q. L., S.Y. L., H. Y. and C.Q. Z. contributed to surgery performance on the patients; K.F. S., X.L. Y. and C.Q. Z. contributed to verify the underlying data, interpretation of results and preparation of figures; K.F. S. and C.Q. Z. contributed to draft and revise the manuscript and figures. All authors edited and approved the paper.

Declaration of Competing Interest

The authors declare that they have no competing interests.

Acknowledgments

This work was supported by National Natural Science Foundation of China (No. 81601143, No. 81771217).

Data Sharing Statement

Source data of this study are available on Mendeley Data, V2, doi: 10.17632/kmxdxhjvcz.2.

Supplementary materials

Supplementary material associated with this article can be found, in the online version, at doi:10.1016/j.ebiom.2021.103537.

References

[1] Tellez-Zenteno JF, Hernandez-Ronquillo L. A review of the epidemiology of temporal lobe epilepsy. Epilepsy Res Treat 2012;2012:630853.
[2] Stolting G, Fischer M, Fahlke C. CLC channel function and dysfunction in health and disease. Front Physiol 2014;5:378.
[3] Nilius B, Droogmans G. Amazing chloride channels: an overview. Acta Physiol Scand 2003;177(2):119–47.
[4] Jentsch TJ, Stein V, Weinreich F, Zdebik AA. Molecular structure and physiological function of chloride channels. Physiol Rev 2002;82(2):503–68.
[5] Jentsch TJ, Pusch M. CLC Chloride Channels and Transporters: Structure, Function, Physiology, and Disease. Physiol Rev 2018;98(3):1493–590.
[6] Kawasaki M, Uchida S, Monkawa T, et al. Cloning and expression of a protein kinase C-regulated chloride channel abundantly expressed in rat brain neuronal cells. Neuron 1994;12(3):597–604.
[7] Jentsch TJ, Friedrich T, Schriever A, Yamada H. The CLC chloride channel family. Pflugers Arch 1999;437(6):783–95.
[8] Dickerson LW, Bonthius DJ, Schutte BC, et al. Altered GABAergic function accompanies hippocampal degeneration in mice lacking ClC-3 voltage-gated chloride channels. Brain Res 2002;958(2):227–50.
[9] Stobrawa SM, Breiderhoff T, Takamori S, et al. Disruption of ClC-3, a chloride channel expressed on synaptic vesicles, leads to a loss of the hippocampus. Neuron 2001;29(1):185–96.
[10] Blümcke I, Thom M, Aronica E, et al. International consensus classification of hippocampal sclerosis in temporal lobe epilepsy: a Task Force report from the ILAE Commission on Diagnostic Methods. Epilepsia 2013;54(7):1315–29.
[11] Hynd MR, Lewohl JM, Scott HL, Dodd PR. Biochemical and molecular studies using human autopsy brain tissue. J Neurochem 2003;85(3):543–62.
[12] World Medical Association Declaration of Helsinki: ethical principles for medical research involving human subjects. Jama 2013;310(20):2191–4.
[13] Wang Z, Huang K, Yang X, et al. Downregulated GPR30 expression in the epileptogenic foci of female patients with focal cortical dysplasia type IIb and tuberous sclerosis complex is correlated with (18) F-FDG PET-CT values. Brain Pathol 2021;31(2):346–64.
[14] Wu Z, Huo Q, Ren L, et al. Gluconate suppresses seizure activity in developing brains by inhibiting CLC-3 chloride channels. Mol Brain 2019;12(1):50.
[15] Bardoni R, Shen KF, Li H, et al. Pain Inhibits GRPR Neurons via GABAergic Signaling in the Spinal Cord. Sci Rep 2019;9(1):15804.
[16] Bouilleret V, Ridoux V, Depaulis A, Marescaux C, Nehlig A, Le Gal La Salle G. Recurrent seizures and hippocampal sclerosis following intrahippocampal kainate injection in adult mice: electroencephalography, histopathology and synaptic reorganization similar to mesial temporal lobe epilepsy. Neuroscience 1999;89(3):717–29.
[17] Riban V, Bouilleret V, Pham-Lê BT, Fritschy JM, Marescaux C, Depaulis A. Evolution of hippocampal epileptic activity during the development of hippocampal sclerosis in a mouse model of temporal lobe epilepsy. Neuroscience 2002;112(1):101–11.
[18] Oostenveld R, Fries P, Maris E, Schoffelen JM. FieldTrip: Open source software for advanced analysis of MEG, EEG, and invasive electrophysiological data. Computational intelligence and neuroscience 2011;2011:156869.
[19] FreeSurfer Fischl B. NeuroImage 2012;62(2):774–81.
[20] Fedele T, Burnos S, Boran E, et al. Resection of high frequency oscillations predicts seizure outcome in the individual patient. Sci Rep 2017;7(1):13836.
[21] David O, Blauwblomme T, Job AS, et al. Imaging the seizure onset zone with stereo-electroencephalography. Brain 2011;134(Pt 10):2898–911.
[22] Jensen EC. Quantitative analysis of histological staining and fluorescence using ImageJ. Anat Rec (Hoboken) 2013;296(3):378–81.
[23] Faul F, Erdfelder E, Lang AG, G*Power Buchner A. 3: a flexible statistical power analysis program for the social, behavioral, and biomedical sciences. Behav Res Methods 2007;39(2):175–91.
[24] Habela CW, Sontheimer H. Cytoplasmic volume condensation is an integral part of mitosis. Cell Cycle 2007;6(13):1613–20.
[25] Olsen ML, Schade S, Lyons SA, Amaral MD, Sontheimer H. Expression of voltage-gated chloride channels in human glioma cells. The Journal of neuroscience: the official journal of the Society for Neuroscience 2003;23(13):5572–82.
[26] Maroso M, Balosso S, Ravizza T, et al. Toll-like receptor 4 and high-mobility group box-1 are involved in ictogenesis and can be targeted to reduce seizures. Nat Med 2010;16(4):413–9.
[27] Ramteke VD, Tandan SK, Kumar D, Aruna Devi R, Shukla MK, Ravi Prakash V. Increased hyperalgesia by 5-nitro-2, 3-(phenylpropylamino)-benzoic acid (NPPB), a chloride channel blocker in crush injury-induced neuropathic pain in rats. Pharmacol Biochem Behav 2009;91(3):417–22.
[28] Bragin A, Wilson CL, Engel Jr J. Voltage depth profiles of high-frequency oscillations after kainic acid-induced status epilepticus. Epilepsia 2007;48(5):35–40 **Suppl**.
[29] Zijlmans M, Jiruska P, Zelmann R, Leijten FS, Jefferys JG, Gotman J. High-frequency oscillations as a new biomarker in epilepsy. Ann Neurol 2012;71(2):169–78.
[30] Buzsaki G, Horvath Z, Urioste R, Hetke J, Wise K. High-frequency network oscillation in the hippocampus. Science 1992;256(5059):1025–7.
[31] Stark E, Roux L, Eichler R, Senzai Y, Royer S, Buzsaki G. Pyramidal cell-interneuron interactions underlie hippocampal ripple oscillations. Neuron 2014;83(2):467–80.
[32] Ylinen A, Bragin A, Nadasdy Z, et al. Sharp wave-associated high-frequency oscillation (200 Hz) in the intact hippocampus: network and intracellular mechanisms. The Journal of neuroscience: the official journal of the Society for Neuroscience 1995;15(1 Pt 1):30–46.
[33] Staba RJ. Normal and Pathologic High-Frequency Oscillations. In: th, Noebels JL, Avoli M, Rogawski MA, Olsen RW, Delgado-Escueta AV, eds. Jasper's Basic Mechanisms of the Epilepsies. Bethesda (MD); 2012.
[34] Bragin A, Engel Jr. J, Wilson CL, Fried I, Mathern GW. Hippocampal and entorhinal cortex high-frequency oscillations (100−500 Hz) in human epileptic brain and in kainic acid−treated rats with chronic seizures. Epilepsia 1999;40(2):127–37.
[35] Jirsch JD, Urrestarazu E, LeVan P, Olivier A, Dubeau F, Gotman J. High-frequency oscillations during human focal seizures. Brain 2006;129(Pt 6):1593–608.
[36] Staba RJ, Wilson CL, Bragin A, Fried I, Engel Jr J. Quantitative analysis of high-frequency oscillations (80-500 Hz) recorded in human epileptic hippocampus and entorhinal cortex. J Neurophysiol 2002;88(4):1743–52.
[37] Usui N, Terada K, Baba K, et al. Clinical significance of ictal high frequency oscillations in medial temporal lobe epilepsy. Clinical neurophysiology: official journal of the International Federation of Clinical Neurophysiology 2011;122(9):1693–700.
[38] Cuddapah VA, Turner KL, Seifert S, Sontheimer H. Bradykinin-induced chemotaxis of human gliomas requires the activation of KCa3.1 and ClC-3. The Journal of neuroscience: the official journal of the Society for Neuroscience 2013;33(4):1427–40.
[39] Sorensen AT, Ledri M, Melis M, Nikitidou Ledri L, Andersson M, Kokaia M. Altered Chloride Homeostasis Decreases the Action Potential Threshold and Increases Hyperexcitability in Hippocampal Neurons. eNeuro 2017;4(6).

[40] Cohen I, Navarro V, Clemenceau S, Baulac M, Miles R. On the origin of interictal activity in human temporal lobe epilepsy in vitro. Science 2002;298(5597):1418–21.
[41] Ben-Ari Y, Holmes GL. The multiple facets of gamma-aminobutyric acid dysfunction in epilepsy. Curr Opin Neurol 2005;18(2):141–5.
[42] Pathak HR, Weissinger F, Terunuma M, et al. Disrupted dentate granule cell chloride regulation enhances synaptic excitability during development of temporal lobe epilepsy. The Journal of neuroscience: the official journal of the Society for Neuroscience 2007;27(51):14012–22.
[43] Miles R, Blaesse P, Huberfeld G, Wittner L, Kaila K. Chloride homeostasis and GABA signaling in temporal lobe epilepsy. In: th, Noebels JL, Avoli M, Rogawski MA, Olsen RW, Delgado-Escueta AV, eds. Jasper's Basic Mechanisms of the Epilepsies. Bethesda (MD); 2012.
[44] Huberfeld G, Wittner L, Clemenceau S, et al. Perturbed chloride homeostasis and GABAergic signaling in human temporal lobe epilepsy. The Journal of neuroscience: the official journal of the Society for Neuroscience 2007;27(37):9866–73.
[45] Munakata M, Watanabe M, Otsuki T, et al. Altered distribution of KCC2 in cortical dysplasia in patients with intractable epilepsy. Epilepsia 2007;48(4):837–44.
[46] Munoz A, Mendez P, DeFelipe J, Alvarez-Leefmans FJ. Cation-chloride cotransporters and GABA-ergic innervation in the human epileptic hippocampus. Epilepsia 2007;48(4):663–73.
[47] Li X, Zhou J, Chen Z, Chen S, Zhu F, Zhou L. Long-term expressional changes of Na+ -K+ -Cl- co-transporter 1 (NKCC1) and K+ -Cl- co-transporter 2 (KCC2) in CA1 region of hippocampus following lithium-pilocarpine induced status epilepticus (PISE). Brain Res 2008;1221:141–6.
[48] Wan L, Chen L, Yu J, et al. Coordinated downregulation of KCC2 and GABA(A) receptor contributes to inhibitory dysfunction during seizure induction. Biochem Biophys Res Commun 2020;532(3):489–95.
[49] Ogren JA, Wilson CL, Bragin A, et al. Three-dimensional surface maps link local atrophy and fast ripples in human epileptic hippocampus. Ann Neurol 2009;66(6):783–91.
[50] Buzsáki G, Horváth Z, Urioste R, Hetke J, Wise K. High-frequency network oscillation in the hippocampus. Science 1992;256(5059):1025–7.
[51] Staba RJ, Bragin A. High-frequency oscillations and other electrophysiological biomarkers of epilepsy: underlying mechanisms. Biomark Med 2011;5(5):545–56.